Topography of Polymer Chains Grafted on a Polymer Surface Underwater

Emiko Uchida† and Yoshito Ikada*

Research Center for Biomedical Engineering, Kyoto University, Kawahara-cho, Shogoin, Sakyo-ku, Kyoto 606 Japan

Received November 8, 1996; Revised Manuscript Received April 9, 1997[⊗]

ABSTRACT: The topography of water-soluble polymer chains immobilized on a rigid polymer surface underwater was studied using atomic force microscopy (AFM). As the substrate polymer a smooth poly(ethylene terephthalate) (PET) film was employed and polymer chains of various lengths were chemically immobilized by surface graft polymerization of 2-(dimethylamino)ethyl methacrylate onto the film using the UV-induced graft polymerization method. The degree of polymerization (N) of graft chains ranged from 28 to 960. Except for the shortest chains ($N = 28$) the graft polymer chains were found to stretch out on the substrate underwater, forming a brush structure. The graft layers exhibited inhomogeneous structure, that is, clusters. This cluster formation was ascribed to substantially poor solvency of water for the graft polymer chain. AFM scanning performed at varying loads from 0.25 to 10 nN underwater revealed that, with the increasing graft chain length, AFM images underwater exhibited deformation (tilting) of the clusters at loads higher than 2.5 nN, unlike those in air. When a fixed area of the grafted surface was subjected to cyclic scanning, the tilting direction of clusters was completely in accordance with the scanning direction, and the image of tilting clusters was reproducible. This suggests that the tilting of clusters is reversible, recovering to the previous unperturbed shape as soon as the loading tip has been taken away. The lateral structure of the polymer chains grafted onto the smooth surface underwater was compared with that predicted by brush theories.

Introduction

A thin layer of polymer chains chemically attached by one end to a polymer substrate (polymer brushes) can dramatically affect the surface properties of polymer substrate such as adhesion,[1,2] lubrication,[3,4] wettability,[5,6] friction,[7,8] and biocompatibility.[9,10] Most of the basic studies on these systems have been devoted to determination of the brush chain configuration in good and Θ solvents.[11−22]

Theoretical treatments to identify the structure of end-grafted chains in *poor solvent* have been attempted recently by Lai and Binder,[23] Grest and Murat,[24] and Balazs et al.[25−27] These studies predict that end-grafted chains clump together in a sufficiently poor solvent to form a "dimpled" layer in which the depth of the dimples and the distance between them depend on the graft chain length and density. These theoretical predictions were compared with experimental studies on layers adsorbed with diblock copolymers using atomic force microscopy (AFM).[28−30] The AFM image of adsorbed layers scanned *in air*, which can be considered as a poor solvent for polymers, revealed formation of dimples, densely packed clusters, or lateral inhomogeneities composed of more than one polymer chain. Transition from dimples to isolated islands was observed by decreasing the graft density, in agreement with the theoretical predictions.

The majority of published studies have focused on characterizing the layers at the static equilibrium, but actual properties of graft polymer chains may be governed not only by their static structure but also by their dynamic behavior. So far, we have only limited information on the dynamic aspects of polymer brushes in both theoretical and experimental studies. Rabin and Alexander,[31] Mioa et al.,[32] and Lai and Binder[33] have theoretically studied the properties of polymer brushes in equilibrium with a good solvent under shear flow. It was found that the solvent shear flow caused chain tilting toward and stretching along the direction of the flow, whereas the overall conformational properties in the direction normal to that of the flow remained essentially unaffected. To our knowledge, experimental evidence in this area is lacking, except for a recent study on the collective motion of adsorbed diblocks carried out using dynamic light scattering.[34]

Table 1. Weight-Average Molecular Weight (M_W), Degree of Polymerization (N), Average Interchain Distance (d), and Radius of Gyration of Graft Chains in Θ-Solvent ($R_g^Θ$)

polymer code	M_W	N	d/nm	$R_g^Θ$/nm
Gr-4	4400	28	1.7	2.6
Gr-22	22000	140	1.2	5.9
Gr-90	90000	570	1.9	12.0
Gr-125	125000	800	1.7	14.0
Gr-150	150000	960	1.4	16.0

The objective of the present work is to study the dynamic behavior and lateral structure of polymer brushes *chemically* grafted on a *polymer* substrate underwater using AFM. Most of the polymer brushes studied hitherto are not chemically grafted to polymeric substrates. As mentioned above, the lateral structure of polymer brushes formed by *physically* adsorbed diblocks in air has been investigated with the AFM method.[29,30] An advantage of using the chemically immobilized chains for this type of research is that a whole spectrum of solvents (from poor to good) can be utilized without desorption of chain brushes from the polymer substrate. A poly(ethylene terephthalate) (PET) film and 2-(dimethylamino)ethyl methacrylate (DMAEMA) are used in the present study as the polymer substrate and monomer for graft polymerization, respectively. We have previously demonstrated that a tailored PET surface with varying graft chain lengths

* To whom correspondence should be addressed. Telephone: (075) 751-4115. FAX: (075) 751-4144. E-mail: yyikada@medeng.kyoto-u.ac.jp.

† On leave from Kacho Junior College, Kyoto, Japan.

⊗ Abstract published in *Advance ACS Abstracts,* August 15, 1997.

S0024-9297(96)01660-9 CCC: $14.00

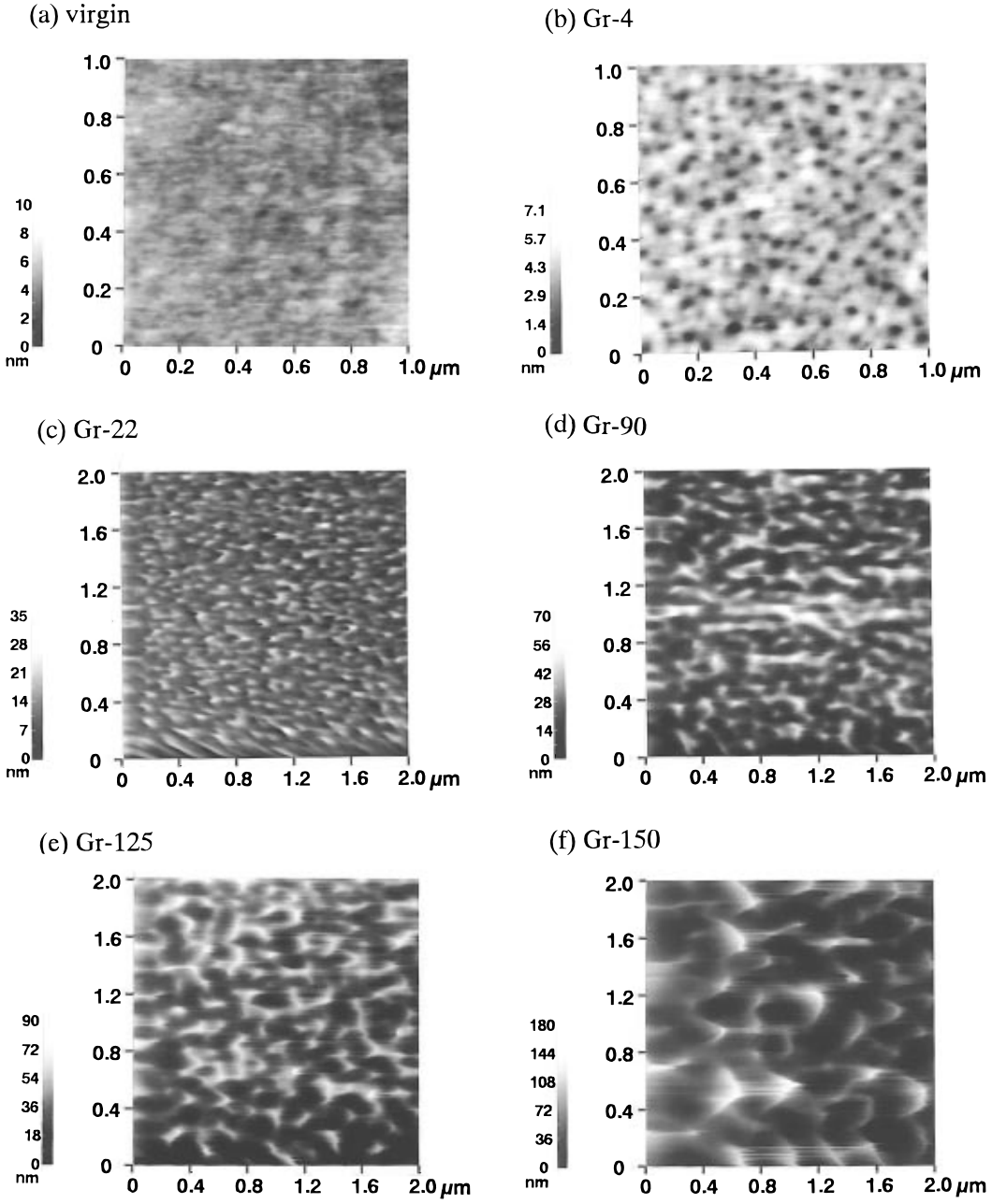

Figure 1. AFM image of film surfaces grafted with different lengths of polyDMAEMA chains (5 nN load, 2 μm/s scanning speed, and 2 × 2 μm^2 scan area except for a and b (1 × 1 μm^2)). Brighter areas indicate higher levels.

and densities can be obtained by changing the DMAEMA concentration and UV irradiation time, respectively.[35]

Experimental Section

Materials. An axially oriented PET film of 100 μm thickness was kindly provided by Teijin Co., Ltd., Tokyo, Japan. For purification it was subjected to Soxhlet extraction with methyl alcohol for 20 h. The mean surface roughness of the virgin PET film was 2.3 nm when measured at an area of 5 × 5 μm^2 using AFM. The cationic DMAEMA monomer was supplied by Mitsubishi Gas Chemical Co., Ltd., Tokyo, Japan. Sodium 4-(2-hydroxy-1-naphthylazo)benzenesulfonate (C. I. Acid Orange 7, Tokyo Kasei Co., Ltd., Japan, λ_{max} 485 nm) was purified with the Robinson-Mills method. *meta*-Sodium periodate ($NaIO_4$) as well as other reagents were used as obtained.

Surface Graft Polymerization. Graft polymerization of the DMAEMA monomer onto the PET film was performed with the simultaneous UV irradiation method without photosensitizers and degassing.[36] Briefly, a strip of PET film was placed in a Pyrex glass ampule with an excess of aqueous monomer solution containing 5 × 10^{-4}M $NaIO_4$. The film and monomer mixture in the ampule were exposed to UV radiation from a 1000 W high-pressure mercury lamp (2537−5791 Å Riko rotary RH400-10 w type, Riko Co., Ltd., Tokyo, Japan). After

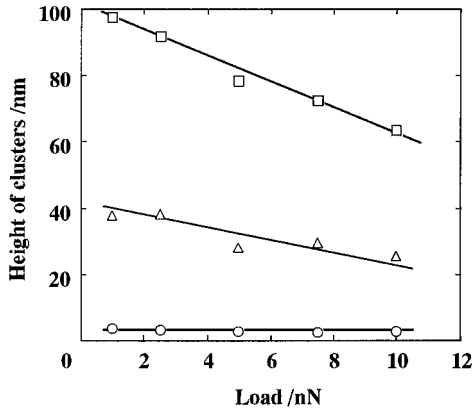

Figure 2. Effect of scanning load on the height of clusters for three samples: (○) Gr-4; (△) Gr-90; and (□) Gr-150.

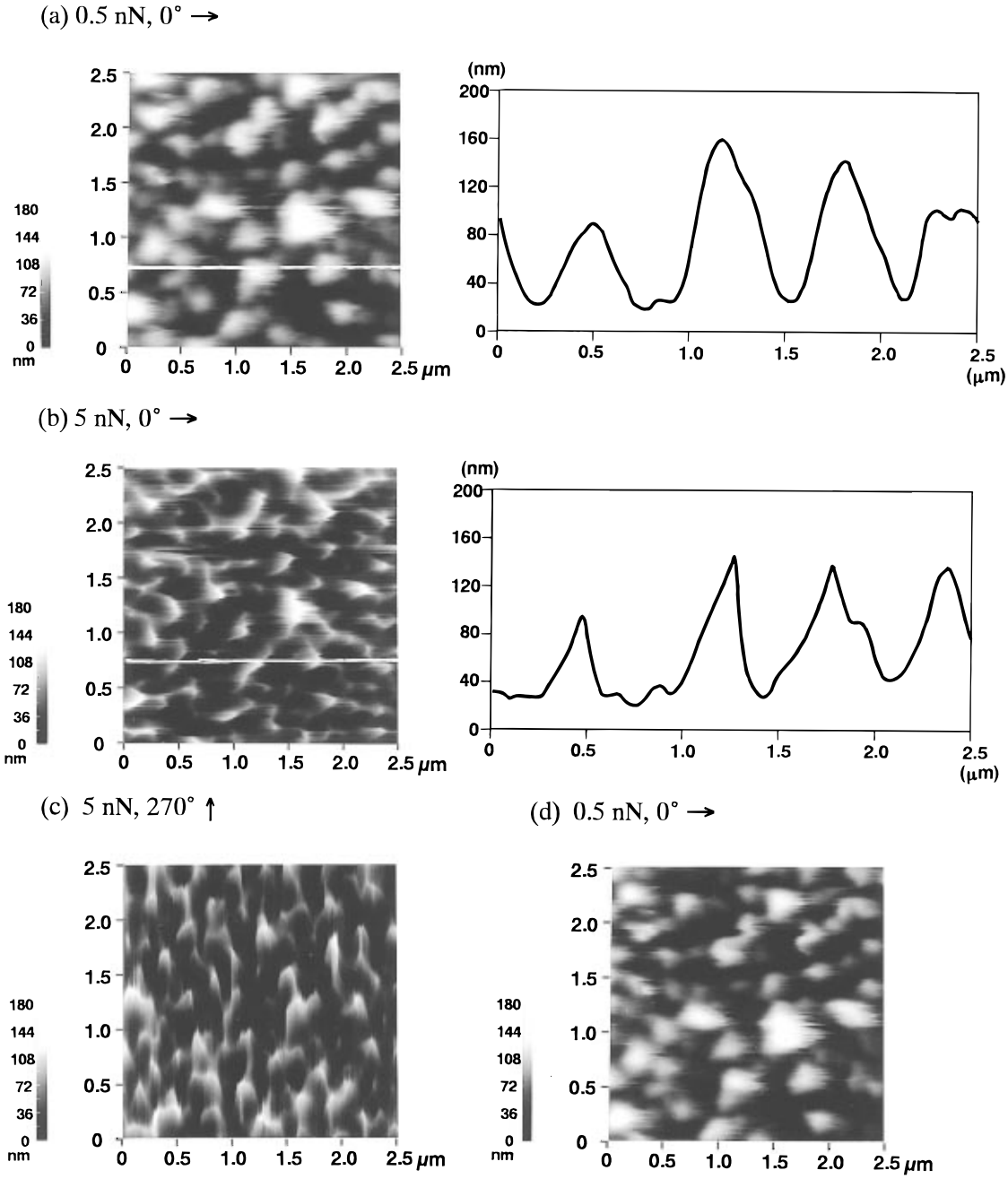

Figure 3. Effect of scanning direction on the cluster deformation for Gr-150. The scanning order is a → b → c → d (2.5 μm/s scanning speed and 2.5 × 2.5 μm^2 scan area). The normal load and scanning angle direction are indicated in the figures. The cross section corresponds to the line drawn in the image.

UV irradiation, the film was immersed in plenty of distilled water under continuous stirring for 20 h at 25 °C to remove the homopolymer formed. The density of polyDMAEMA chains grafted onto the PET film was determined by colorimetry, as described elsewhere.[36] Table 1 shows characteristics of the grafted films used in this work. The weight-average molecular weight of graft chains was estimated from that of the homopolymer formed in the outer solution during graft polymerization. The radius of gyration of the graft chains in Θ-solvent (R_g^{Θ}) was estimated from the eq 1, where a is the

$$R_g^{\Theta} = aN^{1/2} \quad (1)$$

statistical segment length and N is the degree of polymerization of graft chains. The segment length of polyDMAEMA was assumed to be 0.5 nm, which is the segment length of sodium poly(styrene sulfonate),[37] because both the polymers are ionic. The average interchain distance (d) was experimentally determined to be 1.6 nm.[35]

AFM Measurement. A commercial instrument, Olympus NV 2000 (Olympus Optical Co., Ltd., Tokyo, Japan) equipped with an atomic head of 30 × 30 μm^2 scan range was used for AFM measurements of the grafted surface. AFM scanning was performed in air or underwater in the constant force mode using a V-shaped Si_3N_4 cantilever covered with gold on the back for laser beam reflection (OMOL-TR 400 PS microcantilever). Two cantilevers with nominal spring constants of 0.02 and 0.09 N m^{-1} were used underwater and in air, respectively. The tip of both the cantilevers had a pyramidical form with the end radius of curvature less than 20 nm. The water used throughout this study was deionized, double distilled, and particle-free and had pH of 6.2.

Results and Discussion

Topographical Observation Underwater. Figure 1 presents surface topographical images of the films having graft polymer chains of different lengths. They were scanned underwater at a normal force of 5 nN which gave a stable image in air without any appreciable damage to the film surface. Unless otherwise

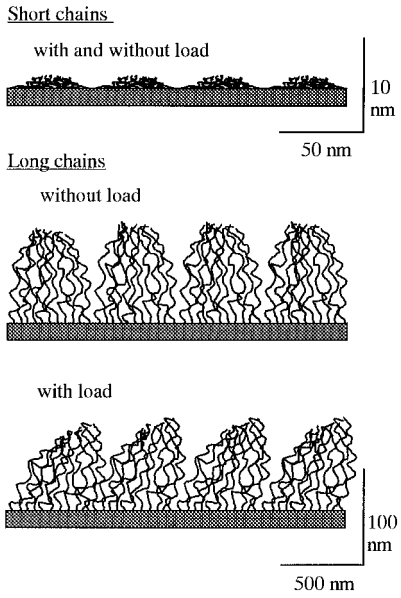

Figure 4. Topographical models for short and long graft chains underwater.

noted, the scanning direction was from left to right. White and dark regions represent topographically higher and lower levels, respectively. These AFM images were reproducible, as scanning on different regions in the same sample gave an identical image over 2 × 2 μm^2. In addition, no image differences were observed among various samples of the same graft chain length and density. The surface of the grafted film having the shortest chain length (Gr-4) seems to have laterally inhomogenous structure, *clusters* (Figure 1b). This inhomogeneous structure clearly resembles the feature obtained from a numerical mean field analysis by Balazs et al.[26] in a poor solvent. The size of clusters estimated from the Gr-4 image is 48 nm wide and 3 nm high, and the distance between them is approximately 50 nm. Interestingly, a similar AFM image was reported by Siqueira et al.[30] for end-functionalized polystyrene brushes in air. They ascribed this inhomogeneous structure to aggregation of polymer chains under the poor solvent condition. Water is a poor solvent for this DMAEMA polymer, which is amphiphilic in nature and has a lower critical solution temperature around 45 °C.[35] Another example of poor solvency of water for grafted water-soluble polymers was reported by Stipp.[38] Stipp observed a mica surface with poly(acrylic acid) (PAA) adsorbed from aqueous solution using scanning force microscopy and demonstrated that water is a relatively poor solvent even for the protonated PAA chain at the PAA concentration used (PAA 8 ppm in 1.00 mM HCl).

As the graft chain length increased, the clusters became higher and displayed *tilting* toward scan direction, as can be seen in Figure 1c through 1f (Gr-22 through Gr-150). Such tilting of polymer brushes has been theoretically predicted to occur under solvent shear flow in good solvents.[31−33] It is likely that the observed *cluster tilting* is a consequence of the mechanical stress applied by friction of the tip on polymer molecules underwater. To confirm this presumption, we performed AFM scanning at loads varying from 0.25 to 10 nN on the grafted surfaces. Clusters clearly tilted for Gr-150 at loads above 2.5 nN, whereas no deformation was seen for Gr-4 even at a 10 nN load (data not shown). The height of clusters estimated from the cross section of topographical images is shown in Figure 2. The cluster height decreases linearly with an increase in load except for Gr-4. To ascertain whether or not the cluster tilting is reversible, the same area of grafted surface was subjected to cyclic scanning at 0.5 and 5 nN loads. Figure 3 shows the result, together with the effect of scan direction on the cluster deformation for Gr-150. Scanning in the directions of right, down, left, and up is indicated as 0, 90, 180, and 270°, respectively. Parts a and d of Figure 3 show the images both scanned at 0° direction and 0.5 nN load, but the former is the image of the first scan while the latter is that of the last scan performed after scanning at all the angle directions. As can be seen from Figure 3, the tilting direction of clusters coincides with the scanning direction. It should be also noted that there is no image difference between parts a and d of Figure 3. These AFM images were very reproducible, regardless of the scanning speed. This finding is in contrast to that of Rädler et al,[39] who reported that any stable images could not be obtained at lower scanning speeds because the tip penetrated through the fluid layer. This suggests that the tilting of clusters is temporary, recovering to the previous unperturbed shape as soon as the loading tip has been taken away and is not raveled by friction of the tip. This result may be ascribed to the much more viscous state of DMAEMA polymer clusters.

Plausible topographies of graft polymer chains underwater are schematically illustrated in Figure 4, referring to the above AFM images and cross sections.

Thickness of the Graft Layer. To get deeper insight into the configuration of graft polymer chains underwater, we synthesized partially grafted surfaces by partially shielding the PET film from UV with a thin metal plate during graft polymerization. Figure 5 shows the image and cross section at the boundary between the grafted and the ungrafted, shielded area underwater. The observed AFM images were obtained at 0.5 nN load, where no appreciable cluster deformation

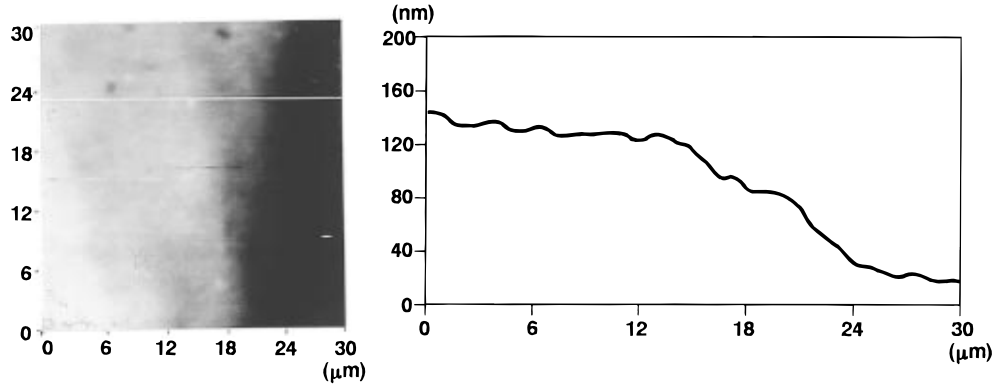

Figure 5. AFM image and cross section at the boundary between the grafted and the ungrafted area. (0.5 nN load, 15 μm/s scanning speed, and 30 × 30 μm^2 scan area).

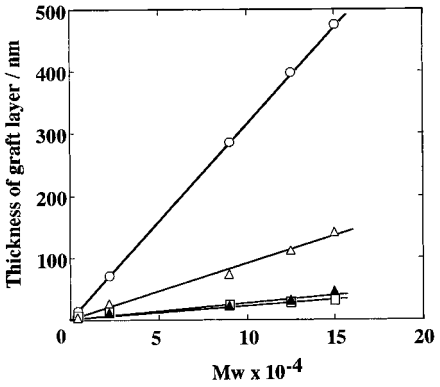

Figure 6. Thickness of graft layer as a function of the molecular weight (M_w) of graft chains: (○) full contour length of graft chains (N_a); (△) thickness of graft layer underwater (L_{water}); (▲) thickness of graft layer in air (L_{air}); (□) two times the radius of gyration of graft chains in a Θ-solvent ($2R_g^{\Theta}$).

occurred. The cross section corresponds to the line drawn in the image. From the cross section underwater and in air, we can evaluate the thickness of graft layer, L_{water} and $L_{air,}$ respectively. We could not obtain the L_{air} for Gr-4, because the boundary between the grafted and the ungrafted area was indistinguishable in this case.

As mentioned above, the observed strong tendency for the graft chains to aggregate into clusters seems to be due to poor solvency of water for this polymer. The volume fraction of monomer unit within the graft layer (φ) underwater can be calculated from eq 2[18] using the observed L_{water}:

$$\varphi = Na^3/d^2L_{water} \qquad (2)$$

The φ value was found to be 0.3 for every layer, irrespective of the graft chain length, indicating that the monomer unit concentration within the graft layer is very high. The full contour length of chain (Na), L_{air}, $L_{water,}$ and $2R_g^{\Theta}$ are plotted against the molecular weight of graft chains in Figure 6. Even though the fluctuation of R_g^{Θ} is presumed to be ± 50%, their size order is as follows:

$$Na >> L_{water} >> L_{air} \approx 2R_g^{\Theta} \qquad (3)$$

These relations suggest that water is a poor solvent of DMAEMA polymer but is not as poor as "air" for this polymer.

Topographical Observation of Clusters. As represented in Figure 1, the cluster image of polymer brushes was observed underwater. It seems as if the clusters are undeformed or without tilting at low loads, but one cannot deny that they are completely undeformed by scanning underwater. Therefore, we attempted to fix the cluster shape in air by staining a partially grafted surface with an anionic dye to form ion complex between the polymer brushes and the dye molecules. As is shown in Figure 7, AFM observation of the stained surface in air exhibited a clear boundary between the grafted layer and a bare surface and distinctly the cluster structure near the boundary, but such a clear boundary could not be seen when the surface was covered with short polymer chains or without dyeing. Comparison of Figure 7 with the cross section shown in Figure 5, which does not display a precipitous cliff, but only a gentle slope, reveals that the surface shown in Figure 7 is covered with polymer chains having a graft density gradient. The surface with such a graft density gradient seems to have been created by UV irradiation with an intensity gradient at the boundary area, made by the thin metal plate placed on the PET film to partially shield the UV light. The height of the clusters in Figure 7 increased with

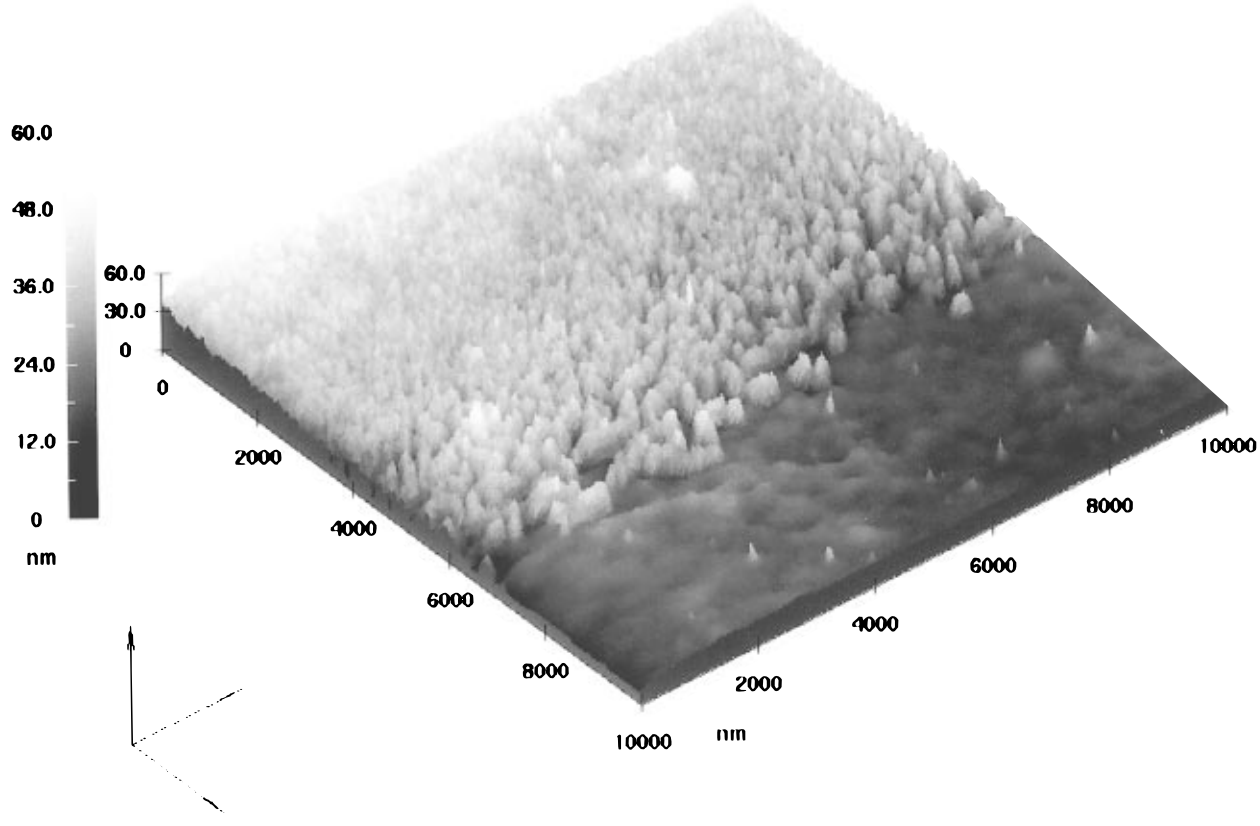

Figure 7. AFM image in air of a partially grafted surface stained with an anionic dye to form the ion complex (5 nN load, 1 μm/s scanning speed, and 1 × 1 μm^2 scan area).

the graft density, being, for instance, 30 and 85 nm at a low and a high density area, respectively. This result is in good agreement with that predicted by Auroy et al.[16] In their work, the chains at a low graft density had flat conformation in poor solvent, spreading onto the surface. As the spacing between anchor points became sharper, the thickness of the interface increased, owing to mutual interchain interactions. At a high graft density, graft chains stretched themselves, yielding polymer brushes.

Conclusions

Except for the shortest chains, the DMAEMA polymer chains chemically grafted on the PET substrate were found by AFM observation underwater to stretch out on the substrate surface, forming a brush structure. The graft layers exhibited inhomogeneous cluster structure. AFM scanning was performed at varying loads from 0.25 to 10 nN underwater. With the increasing graft chain length, AFM images above 2.5 nN load exhibited more remarkable deformation (tilting) of clusters underwater, unlike those in air. When a fixed area of grafted surface was subjected to cyclic scanning, the tilting direction of clusters completely obeyed the scanning direction. The tilting of clusters was reversible, recovering to the previous unperturbed shape as soon as loading tip had been taken away. The thickness of the graft layer estimated from the cross section in air and underwater (L_{air} and L_{water}) and the radius of gyration of the graft chain in Θ-solvent (R_g^{Θ}) was in the following order:

$$L_{water} >> L_{air} \approx 2R_g^{\Theta}$$

This order suggests that water acts as a poor solvent but is not as poor as air for the polyDMAEMA chains grafted onto the PET film.

Acknowledgment. We thank Dr. O. N. Tretinnikov of B. I. Stepanov Institute of Physics, Academy of Sciences of Belarus, for helpful discussions.

References and Notes

(1) Lee, Y. M.; Ihm, S. Y.; Shim, J. K.; Kim, J. H.; Cho, C. S.; Sung, Y. K. *Polymer* **1995**, *36*, 81.
(2) Bai, G.; Hu, X.; Yan, Q. *Polym. Bull.* **1996**, *36*, 503.
(3) Uyama, Y.; Tadokoro, H.; Ikada, Y. *J. Appl. Polym. Sci.* **1990**, *39*, 489.
(4) Inoue, H.; Uyama, Y.; Uchida, E.; Ikada, Y. *Cell Mater.* **1992**, *2*, 21.
(5) Ruckert, D.; Geuskens, G. *Eur. Polym. J.* **1996**, *32*, 201.
(6) Hamilton, L. M.; Green, A.; Edge, S.; Badyal, J. P. S.; Feast, W. J.; Pacynko, W. F *J. Appl. Polym. Sci.* **1994,** *52*, 413.
(7) Uyama, Y.; Tadokoro, H.; Ikada, Y. *Biomaterials* **1991**, *12*, 71.
(8) Tomita, N.; Tamai, S.; Okajima, E.; Hirao, Y.; Ikeuch, K.; Ikada, Y. *J. Appl. Biomater.* **1994**, *5*, 175.
(9) Nakayama, Y.; Matsuda, T.; Irie, M. *ASAIO J.* **1993**, M542.
(10) Kulik, E.; Ikada, Y. *J. Biomed. Mater. Res.* **1996**, *30*, 295.
(11) de Gennes, P. G. *Macromolecules* **1980**, *13*, 1069.
(12) Milner, S. T.; Witten, T. A.; Cates, M. E. *Macromolecules* **1988**, *21*, 2610.
(13) Murat, M.; Grest, G. S. *Macromolecules* **1989**, *22*, 4054.
(14) Lai, P. Y.; Halperin, A. *Macromolecules* **1991**, *24*, 4981.
(15) Milner, S. T. *Science* **1991**, *251*, 905.
(16) Auroy, P.; L. Auvray; Leger, L. *Macromolecules* **1991**, *24*, 5158.
(17) Auroy, P.; L. Auvray *Macromolecules* **1992**, *25*, 4134.
(18) Halperin, A.; Tirrell, M.; Lodge, T. P. *Adv. Polym. Sci.* **1992**, *100*, 31.
(19) Field, J. B.; Toprakcioglu, C.; Ball, R. C.; Stanley, H. B.; Dai, L.; Barford, W.; Penfold, J.; Smith, G.; Hamilton, W. *Macromolecules* **1992**, *25*, 434.
(20) Israels, R.; Scheutjens, J. M. H. M.; Fleer, G. J. *Macromolecules* **1993**, *26*, 5405.
(21) Dan, N.; Tirrell, M. *Macromolecules* **1993**, *26*, 4310.
(22) Grest, G. S. *Macromolecules* **1994**, *27*, 418.
(23) Lai, P. -Y.; Binder, K. *J. Chem. Phys.* **1992**, *97*, 586.
(24) Grest, G.; Murat, M. *Macromolecules* **1993**, *26*, 3108.
(25) Huang, K.; Balazs, A. C. *Macromolecules* **1993**, *26*, 4736.
(26) Yeung, C.; Balazs, A. C.; Jasnow, D. *Macromolecules* **1993**, *26*, 1914.
(27) Gersappe, D.; Fasolka, M.; Balazs, A. C. *J. Chem. Phys.* **1994**, *100*, 9170.
(28) O'Shea, S. J.; Welland, M. E.; Rayment, T. *Langmuir* **1993**, *9*, 1826.
(29) Zhao, W.; Krausch, G.; Rafailovich, M. H.; Sokolov, J. *Macromolecules* **1994**, *27*, 2933.
(30) Siqueira, D. F.; Kohler, K.; Stamm, M. *Langmuir* **1995**, *11*, 3092.
(31) Rabin, Y.; Alexander, S. *Europhys. Lett.* **1990**, *13*, 49.
(32) Miao, L.; Guo, H.; Zuckermann, M. J. *Macromolecules* **1996**, *29*, 2289.
(33) Lai, P.-Y.; Binder, K. *J. Chem. Phys.* **1993**, *98*, 2366.
(34) Fytas, G.; Anastasiadis, S. H.; Seghrouchni, R.; Vlassopoulos, D.; Li, J.; Factor, B. J.; Theobald, W.; Toprakcioglu, C. *Science* **1996**, *274*, 2041.
(35) Uchida, E.; Uyama, Y.; Ikada, Y. *Langmuir* **1994**, *10*, 1193.
(36) Uchida, E.; Uyama, Y.; Ikada, Y. *J. Appl. Polym. Sci.* **1990**, *41*, 677.
(37) Amiel, C.; Sikka, M.; Schneider, J. W.; Jr. Tsao,.Y.-H.; Tirrell, M.; Mays, J. W. *Macromolecules* **1995**, *28*, 3125.
(38) Stipp, S. L. *Langmuir* **1996**, *12*, 1884.
(39) Rädler, J.; Radmacher, M.; Gaub, H. E. *Langmuir* **1994**, *10*, 3111.

MA961660K